

Simple full-range carrier frequency offset estimation for high speed CO-OFDM

Hae Young Rha,^{1,2*} Chun Ju Youn,² Eun Soo Nam,² and Hae-Wook Choi¹

¹Department of Electrical Engineering, Korea Advanced Institute of Science and Technology (KAIST), Daejeon, South Korea

²Photonic/Wireless Convergence Components Department, Electronics and Telecommunications Research Institute, 138 Gajeongno, Yuseong-gu, Daejeon, South Korea
miroandi@kaist.ac.kr

Abstract: We propose a simple, full-range carrier frequency offset (CFO) algorithm for coherent optical orthogonal frequency division multiplexing (CO-OFDM) systems. By applying the Chinese remainder theorem (CRT) to training symbol of single frequency, the proposed CFO algorithm has wide range with shorter training symbol. We numerically and experimentally demonstrate the performance of CRT-based algorithms in a 16-ary quadrature amplitude modulation (QAM) CO-OFDM system. The results show that the estimation range of the CRT-based algorithm is full-range corresponding to the sampling frequency. Also, the bit error ratio (BER) degradation of the proposed algorithm with one training symbol is negligible. These results indicate that the proposed algorithm can be used as a wide range CFO estimator with an increased data rate in high speed CO-OFDM systems.

©2013 Optical Society of America

OCIS codes: (060.1660) Coherent communications; (060.2330) Fiber optics communications.

References and links

1. W. Shieh and C. Athaudage, "Coherent optical orthogonal frequency division multiplexing," *Electron. Lett.* **42**(10), 587–589 (2006).
2. Optical Internetworking Forum, "Integrable tunable transmitter assembly multi source agreement," OIF-ITTA-MSA-01.0, Nov. (2008).
3. T. M. Schmidl and D. C. Cox, "Robust frequency and timing synchronization for OFDM," *IEEE Trans. Commun.* **45**(12), 1613–1621 (1997).
4. C. J. Youn, X. Liu, S. Chandrasekhar, Y.-H. Kwon, J.-H. Kim, J. S. Choe, D. J. Kim, K. S. Choi, and E. S. Nam, "Channel estimation and synchronization for polarization-division multiplexed CO-OFDM using subcarrier/polarization interleaved training symbols," *Opt. Express* **19**(17), 16174–16181 (2011).
5. Z. Wang, Y. Qiao, and Y. Ji, "A novel joint frequency offset and channel estimation method for CO-OFDM system," *Communications and Photonics Conference and Exhibition (ACP)* 607–608 (2010).
6. S. Cao, S. Zhang, Y. Shaoliang, K. Changyuan, and P.-Y. Kam, "Full range pilot-assisted frequency offset estimation for OFDM systems," in *Proceedings of OFC'13*, paper JW2A.53.
7. X.-H. Fan, J. Yu, D. Qian, and G.-K. Chang, "A fast and efficient frequency offset correction technique for coherent optical orthogonal frequency division multiplexing," *J. Lightwave Technol.* **29**(13), 1997–2004 (2011).
8. X. Zhou, K. Long, R. Li, X. Yang, and Z. Zhang, "A simple and efficient frequency offset estimation algorithm for high-speed coherent optical OFDM systems," *Opt. Express* **20**(7), 7350–7361 (2012).
9. H. Y. Rha, B. G. Jeon, and H. Choi, "Simple wide range carrier frequency offset estimation for coherent optical OFDM," *IEEE Photon. Technol. Lett.* **24**(22), 2064–2066 (2012).
10. M. Lei, M. Zhao, J. Zhong, and Y. Cai, "ML-based estimation algorithm of frequency offset for 2×2 STBC-OFDM systems," *ETRI J.* **34**(3), 458–461 (2012).
11. P. H. Moose, "A technique for orthogonal frequency division multiplexing frequency offset correction," *IEEE Trans. Commun.* **42**(10), 2908–2914 (1994).
12. R. Bouziane, R. Koutsoyannis, P. Milder, Y. Benlachtar, J. C. Hoe, M. Glick, and R. I. Killey, "Optimizing FFT Precision in Optical OFDM Transceivers," *IEEE Photon. Technol. Lett.* **23**(20), 1550–1552 (2011).
13. L. Xiang, S. Chandrasekhar, Z. Benyuan, P. J. Winzer, A. H. Gnauck, and D. W. Peckham, "448-Gb/s reduced-guard-interval CO-OFDM transmission over 2000 km of ultra-large-area fiber and five 80-GHz-grid ROADMs," *J. Lightwave Technol.* **29**(4), 483–490 (2011).
14. X. Liu and F. Buchali, "Intra-symbol frequency-domain averaging based channel estimation for coherent optical OFDM," *Opt. Express* **16**(26), 21944–21957 (2008).

15. Z. Xian, Y. Xiaolong, L. Rui, and L. Keping, "Efficient joint carrier frequency offset and phase noise compensation scheme for high-speed coherent optical OFDM systems," *J. Lightwave Technol.* **31**(11), 1755–1761 (2013).
 16. W. Shieh, "Maximum-likelihood phase and channel estimation for coherent optical OFDM," *IEEE Photon. Technol. Lett.* **20**(8), 605–607 (2008).
 17. W. Shieh and I. Djordjevic, "Optical communication fundamentals," in *OFDM for Optical Communications*, 1-st ed. (Academic Press, 2009).
 18. C.-H. Yih, "BER analysis of OFDM systems impaired by DC offset and carrier frequency offset in multipath fading channels," *IEEE Commun. Lett.* **11**(11), 842–844 (2007).
-

1. Introduction

Orthogonal frequency division multiplexing (OFDM) technology has been widely used in various digital communications to combat multipath fading. During the past few years, an optical OFDM system has become an attractive technology due to high dispersion tolerance, and high spectral efficiency in long haul transmissions [1].

Although OFDM is invulnerable against dispersion, the OFDM system consisted of multiple subcarriers is sensitive to phase noise and frequency offset which may cause interchannel interference (ICI) between subcarriers. Accordingly, carrier frequency offset (CFO) estimation and compensation are important functions of OFDM systems. Furthermore, CFO is more severe in fiber optic communication than in RF communication due to the laser instability. In a practical system, it is very difficult to maintain the laser frequency with a small frequency offset because commercially available lasers have frequency stability within ± 2.5 GHz [2]. Thus, wide range CFO estimation is essential in coherent optical OFDM (CO-OFDM) systems.

Studies on CFO estimation algorithms have been investigated for OFDM [3–10]. Schmidl and Cox [3] expressed CFO as a sum of the multiples of the subcarrier spacing frequencies and the remainder, which are called the integral and the fractional parts of CFO, respectively. Using these terms, CFO estimation algorithms using training symbols can be categorized into three approaches. The first approach is a fractional part only estimation of which range is the subcarrier spacing frequency. To widen the CFO estimation range, training symbols are divided into even and odd subcarriers [4], in which an algorithm has doubled the estimation range. The algorithms of this approach have high estimation accuracy, but the range is not wide.

The second approach is estimating the integral part of CFO in the frequency domain in addition to the fractional part of the CFO [3, 5, 6]. The integral part of estimation increases the estimation range up to sampling frequency. However, the estimation in the frequency domain causes high hardware latency because CFO compensation is performed in the time domain at the front end of the OFDM receiver. It becomes particularly severe in high speed OFDM systems.

Thus, the integral part of CFO is estimated in the time domain for practical hardware implementation. In this approach the final CFO estimation is obtained by combining several time domain estimations. An algorithm using sample-shifted training symbols [7] and an algorithm using two estimations with different sample intervals [8], were suggested. Also, we recently proposed the Chinese remainder theorem (CRT)-based CFO algorithm [9], of which estimation range is the same as the sampling frequency. These algorithms have wide estimation range, low hardware complexity, and latency; however their training symbol structure is complex and more than one training symbol for CFO estimation could be required.

The purpose of this study is to show experimentally the feasibility of the CRT-based, CFO algorithm with shorter training symbol. To reduce the overhead due to training symbols, we propose a modified CRT-based CFO algorithm using a training symbol with a single frequency. The results of this study may enable full-range CFO estimation with lower overhead in a CO-OFDM system.

A brief review of the principle of the CRT-based CFO algorithm and the theory of the proposed CRT-based algorithm are described in Section 2. To evaluate the proposed system,

experiments were performed. The experimental setup is described in Section 3. Results and discussion are described in Section 4. Finally conclusions are drawn at the end of the paper.

2. Background of the Study

2.1 Background of CRT-based frequency offset estimation

At the receiver in the communication channel with channel noise $\eta(n)$, the sampled baseband signal $r(n)$ with carrier frequency offset (CFO) Δf can be represented by:

$$r(n) = e^{j2\pi n\Delta T_s} s(n) + \eta(n) \quad (1)$$

where $s(n)$ is the signal component and T_s is the sampling period.

To estimate CFO in the time domain, a training symbol consisted of two identical patterns has been used [3]. The frequency offset angle is calculated from the phase differences between identical complex samples. The CFO normalized to $1/(NT_s)$ is estimated by

$$\hat{\varepsilon} = \Delta \hat{f} N T_s = \frac{N}{2\pi L} \text{angle}(P_L), \quad (2)$$

$$P_L = \sum_{m=0}^{L-1} (r(m)^* r(m+L))$$

where $\hat{\varepsilon}$ is the estimated value of normalized CFO, $\text{angle}(\bullet)$ is the phase difference between identical samples, L is the sample interval, N is the size of the inverse fast Fourier transformation (IFFT), and P_L is the correlate function.

In this time domain estimation, the sample interval L determines the accuracy and range of CFO estimation. The estimation range of the normalized CFO is $[-N/2L, N/2L]$ and the variance of normalized CFO is described by Cramér-Rao bound (CRB) [3, 11] as:

$$CRB(\hat{\varepsilon}) = CRB(\Delta \hat{f} N T_s) = \frac{1}{\pi^2} \frac{1}{L \cdot SNR}. \quad (3)$$

The sample interval L can be determined by the tradeoff between the estimation range and accuracy. As the sample interval increases, the accuracy of the estimation also increases, but the range of estimation decreases.

In order to increase the estimation range while retaining high accuracy, the Chinese remainder theorem (CRT) can be applied to CFO estimation as follows. The estimation consists of three time domain estimations with sample interval L_1 , L_2 and L [9]:

$$\hat{\varepsilon}_{L_i} = \frac{L}{2\pi L_i} \text{angle}(P_{L_i}) \quad \text{for } i = 1 \text{ and } 2,$$

$$\hat{\varepsilon}_L = \frac{1}{2\pi} \text{angle}(P_L) \quad (4)$$

where estimated CFOs are normalized to $1/(LT_s)$, L_1 and L_2 are coprime numbers, and L is the product of L_1 and L_2 . Hence, $\hat{\varepsilon}_L$ with longest sample interval L has the highest accuracy among the three estimations.

Two integral parts of normalized CFO can be obtained from quantized $\hat{\varepsilon}_{L_1}$ and $\hat{\varepsilon}_{L_2}$. Then, the extended integral part of the CFO can be uniquely calculated by applying CRT to the two integers as follows.

$$\hat{\varepsilon}_I = \hat{\varepsilon}_{L_1} L_1 (L_1^{-1} \bmod L_2) + \hat{\varepsilon}_{L_2} L_2 (L_2^{-1} \bmod L_1). \quad (5)$$

where mod represent the modular arithmetic. According to CRT, the integer obtained in Eq. (5) has a range of L . The fractional part of CFO with high accuracy $\hat{\epsilon}_F$ is directly obtained from $\hat{\epsilon}_L$. Finally, the estimated CFO $\hat{\epsilon}$ can be described as the sum of the integral and fractional parts of CFO, i.e. $\hat{\epsilon} = \hat{\epsilon}_I + \hat{\epsilon}_F$.

The CRT-based CFO algorithm has accuracy determined by the fractional part. The CFO estimation range is the same as the sampling frequency, because the estimated CFO normalized to $1/(LT_s)$ has the range of L . Accordingly, the CRT-based CFO estimation has full-range and high accuracy.

2.2 Principle of single frequency CRT-based CFO estimation

In the previous CRT-based CFO estimation, the training symbol structure consist of two training symbols with size L as shown in Fig. 1(a). The phase differences between subsymbols S_1, S_2 , and training symbols T_1 are calculated for CFO estimation with the sample interval L_1, L_2 , and L , respectively.

For simpler training symbol structure, a single frequency, CRT-based CFO estimation is proposed as follows. A single frequency signal for training symbol $t(n)$ is described as:

$$t(n) = t_0 e^{jn\phi_s}, \quad \text{for } n = 0, 1, \dots, N_{TS} - 1 \quad (6)$$

where ϕ_s is the phase difference between adjacent samples in the transmitted training symbol, and N_{TS} is the number of training symbol samples. Using Eq. (1) and Eq. (6), the received training symbol is described as:

$$r(n) = t_0 e^{jn(\phi_s + 2\pi\Delta f T_s)} + \eta(n). \quad (7)$$

With a single frequency training symbol, the phase difference between any two samples can be used as a time domain CFO estimation corresponding to the sample interval. For example, CFO estimation with the sample interval L_1 can be obtained from any samples apart L_1 by subtracting the transmitted phase difference, $\phi_s \cdot L_1$ from the measured phase difference. As such, Eq. (4) can be described as:

$$\hat{\epsilon}_{L_i} = \frac{L}{2\pi L_i} (\text{angle}(P_{L_i}) - \phi_s L_i) \quad \text{for } i = 1 \text{ and } 2, \quad (8)$$

$$\hat{\epsilon}_L = \frac{1}{2\pi} (\text{angle}(P_L) - \phi_s L).$$

The rest of calculations are the same as in the previous CRT-based CFO algorithm.

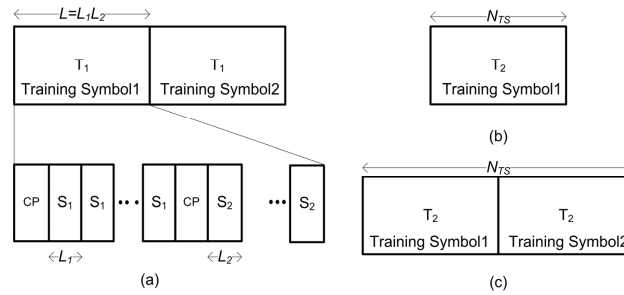


Fig. 1. (a) The training symbol structure for the previous CRT-based CFO algorithm; S_1 , and S_2 are subsymbols and CP is cyclic prefix. The proposed training symbol structure with (b) one, or (c) two training symbols.

Using Eq. (8), any co-prime set can be chosen for L_1 and L_2 , with condition $L_1 \cdot L_2 < N_{TS}$. On the contrary, the product of co-prime set, L , should be the same as the training symbol size, $0.5N_{TS}$, in the previous CRT-based estimation. Also, the previous training symbol

structure consists of two training symbols and requires guard intervals between different subsymbols. Unlike the previous estimation, the proposed CFO estimation does not require a guard interval between the different sample intervals. Also, either one or two training symbols can be used for the proposed algorithm as shown in Fig. 1(b) and 1(c).

For a dual polarization transmission, the training symbol structure can be extended from Fig. 1. The training symbol for each polarization has the same training symbol structure as that of the single polarization and has the same frequency. The polarization rotation would not affect the performance of the proposed algorithm, because the rotation of single frequency does not change the phase difference between the samples. In addition, the proposed training symbol would be invulnerable to chromatic dispersion, because the signal with single frequency does not have frequency dependent group delay difference.

3. Simulation and experimental setup

3.1 Simulation and experiment

In order to evaluate the performance of the proposed CFO algorithm, we numerically and experimentally obtained the bit error rate (BER) and CFO estimation error. Simulations and off-line DSP were performed using MATLAB™. DSP structures of the transmitter and the receiver are shown in Fig. 2(a) and Fig. 2(b), respectively. At the transmitter, a 2^{15} -1 pseudo random binary sequence (PRBS) was mapped to the OFDM subcarriers with 16-ary quadrature amplitude modulation (16 QAM). The mapped signal was transformed to the time domain using IFFT. After cyclic prefix insertion into the time domain signal, training symbols for CFO estimation, symbol synchronization, and channel estimation were attached at the beginning of each OFDM frame. To flatten unequal frequency response magnitude owing to the bandwidth of the channel, pre-emphasis was performed on the waveform. The coefficients for pre-emphasis were obtained from the estimated channel frequency response. Then the pre-equalized waveform was clipped [12] to eliminate unwanted very high amplitude of the signal.

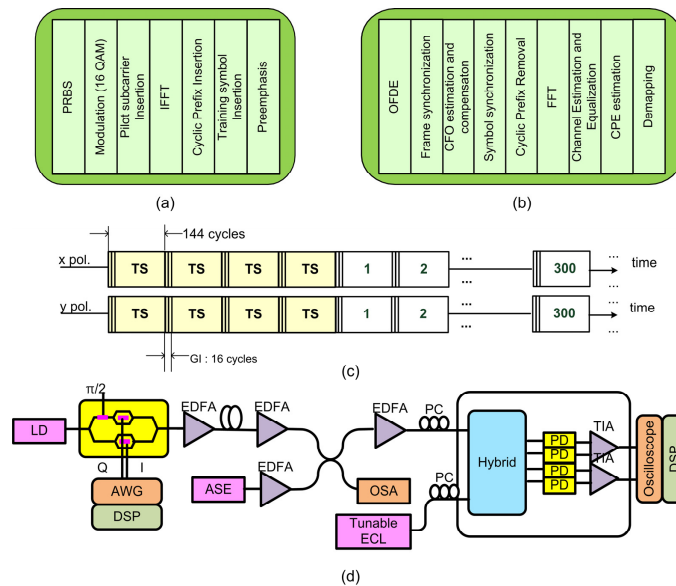


Fig. 2. The schematic of the DSP structures of (a) transmitter, and (b) receiver, (c) frame format for dual polarization and (d) experimental setup; LD: laser diode; EDFA: Erbium-doped fiber amplifier; ASE: Amplified spontaneous emission source; PC: polarization controller; OSA: optical spectrum analyzer; ECL: external cavity laser, OFDE: overlapped frequency domain equalizer, TS: Training symbol for CFO estimation, GI: Guard interval; OFDE was applied only in simulation.

At the receiver, DC offset compensation was applied to the received signal. Then the overlapped frequency domain equalizer (OFDE) [13] was applied to reduce the guard interval in long haul transmission. After OFDE, the start of frame was searched using auto correlation of training symbol then carrier frequency offset was estimated and compensated. Symbol synchronization was performed using correlation between the CFO compensated signal and the known training symbol. The channel response was estimated by zero forcing estimator using training symbols. To reduce the effect of impairment (e.g., the amplified spontaneous emission (ASE) and phase noise), the estimated channel was smoothed using the intra-symbol frequency-domain averaging (ISFA) [14]. Data symbols were equalized and demapped using the estimated channel response and the hard-decision demapper. The common phase error (CPE) due to the residual CFO and phase noise was estimated using pilot subcarriers and compensated in the frequency domain.

An OFDM frame structure consisted of three or four training symbols depending on algorithms and 300 data symbols as shown in Fig. 2(c). A fast Fourier transformation (FFT) size of 128, with the guard interval of 16, was used for the OFDM symbol size of 144. A data symbol consisted of 70 data subcarriers, 6 pilot subcarriers and unused subcarriers. Several innermost and outermost subcarriers were padded with zeros to avoid the effect of phase noise and aliasing noise.

Figure 2(d) shows the experimental setup. An OFDM waveform which was generated by transmitter DSP was stored in an arbitrary waveform generator (AWG) with the sampling rate of 10 GS/s. Analog low pass filters (LPF) of 5 GHz bandwidth were used as smoothing filters, and connected between the AWG and optical modulator. The analog OFDM waveforms were amplified and used to drive an optical I/Q modulator connected to a laser diode (LD) with 100 kHz linewidth. At the receiver the in-phase and quadrature phase signal were sampled using a 40 GS/s oscilloscope with 25 GHz RF bandwidth. The digitized signals were filtered with 10 GHz digital LPF, and resampled and processed at the rate of 10 GS/s by off-line DSP.

3.2 CFO monitoring

Real-time CFO monitoring was applied to get CFO estimation error for the experiment. Since it was difficult to measure the real-time CFO component in the OFDM data, the intentional DC interval between frames was inserted. Thus, real-time CFO monitoring was easily done by applying Fourier transformation to the interval [15] because the DC component moves as much as CFO in the frequency domain. The frequency with a maximum magnitude is the monitored CFO as shown in Fig. 3. At the transmitter, 5000 samples with the rate of 10 GS/s were attached at the head of each OFDM frame and thus, the frequency spacing $f_{spacing}$ was 2MHz. Assuming that the carrier frequency offset was static over one frame and laser linewidth was smaller than the frequency spacing, the monitoring accuracy was $\pm f_{spacing}$ (± 2 MHz). Also, the oscilloscope with the sampling rate of 40 GS/s gave the monitoring range of ± 20 GHz.

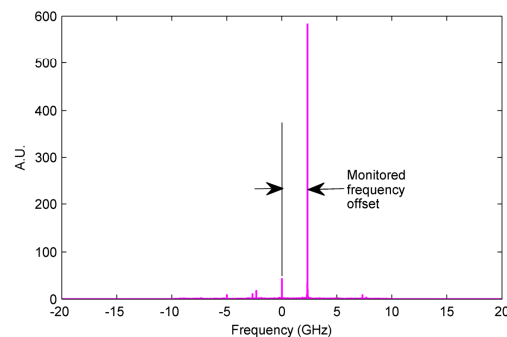


Fig. 3. CFO monitoring in frequency domain.

4. Results and discussion

The mean square estimation error (MSEE) and bit error ratio (BER), as a function of optical signal to noise ratio (OSNR) and the monitored CFO, were obtained for conventional CFO algorithms and for the proposed CFO algorithm; with one or two training symbols for CFO estimation. L_1 of 9, L_2 of 16, and L of 144 were selected for CRT-based algorithms with two training symbols. Also, L_1 of 9, L_2 of 8, and L of 72 were selected for the CRT-based algorithm with one training symbol. The phase difference ϕ_s in Eq. (6) for the proposed training symbol was set to $\pi/4$. Since normalized CFO ε has a different normalization factor for each algorithm, $\text{MSEE}(\phi_{\text{sample}})$ is used instead of $\text{MSEE}(\varepsilon)$, in which ϕ_{sample} is an estimated phase difference between adjacent samples.

4.1 Simulation results

The simulation was performed for the system with 112 Gbps transmission over an 800 km standard single-mode-fiber (SSMF) with polarization division multiplexing 16 quadrature amplitude modulation (PDM 16-QAM). Optical link consisted with 10 spans and each span consisted of 80 km SSMF with a dispersion parameter of 17 ps/nm/km, attenuation α of 0.2 dB/km, and nonlinearity coefficient γ of 1.2 /W/km and EDFA with 16 dB gain. Polarization dispersion D_p was set to 2 ps/ $\sqrt{\text{km}}$. The sampling rate of the simulation was set to 29 GHz to meet the transmission rate of 112 Gbps.

Figure 4 shows the BER as a function of the given CFO. The results show that BER of all CRT-based CFO algorithms was almost the same along the CFO. The simulation results showed the CRT-based algorithms could estimate as much as the sampling frequency. Also, BER of the proposed algorithm showed that the performance degradation due to short training symbol was small.

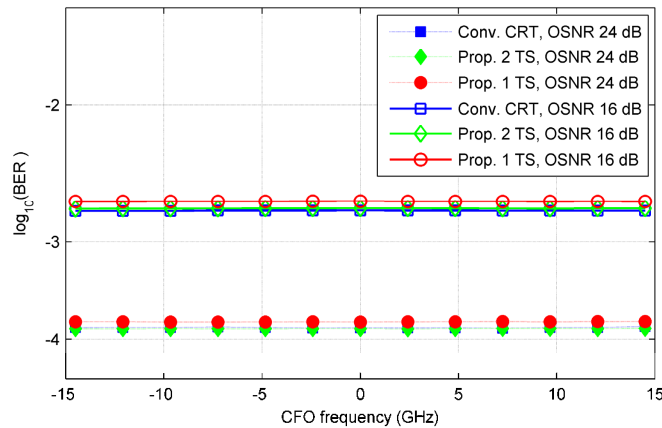


Fig. 4. BER as a function of CFO.

4.2 Experimental results in the absence of CFO

To obtain the estimation error and BER degradation due to CFO estimation, LD was split by beam splitter and used as a local oscillator and a transmit laser for homodyne detection. In the absence of CFO, the given CFO was exactly zero, and the MSEE and OSNR penalty due to CFO estimation error, were obtained as shown in Fig. 5 and Fig. 6.

The MSEE of all algorithms was independent of the OSNR and did not follow Cramér-Rao bound in Eq. (3). In the experiment, the CFO estimation error seemed to be bounded by the phase noise due to the laser linewidth.

The effect of phase noise can be categorized as intercarrier interference (ICI) and common phase error (CPE) [16]. ICI is the interference between subcarriers due to phase noise and can

be considered additive-white-Gaussian-noise (AWGN)-like noise. CPE induces the rotation of channel and can be estimated by pilot-assisted approach. In time domain CFO estimation, CPE between the sample intervals can cause the additive CFO estimation error.

The variance of CFO estimation error due to the CPE between L samples, induced by the laser linewidth $\Delta\nu$, can be described as [17]:

$$\langle \Delta\varphi_{\text{sample}}^2 \rangle = \frac{2\pi\Delta\nu T_s}{L}. \quad (9)$$

Measured MSEE can be compared with the estimation error variance calculated from Eq. (9). For 100 kHz laser linewidth, MSEE due to phase noise of the system with L of 144 and 72 were 4.36×10^{-7} and 8.72×10^{-7} , respectively. The experimental results indicated that laser phase noise could be more influential on CFO estimation than AWGN. Since estimation error variance is proportional to the laser linewidth, a CFO estimation algorithm considering phase noise may be required for higher linewidth, or higher accuracy.

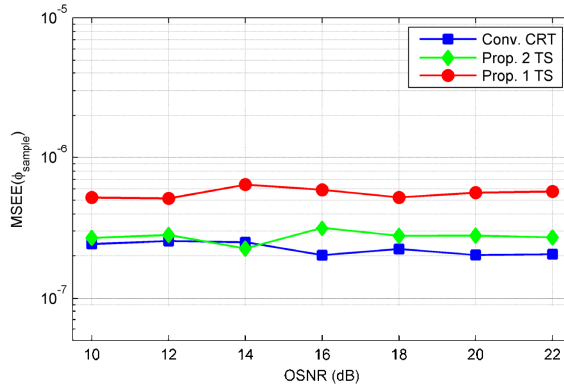


Fig. 5. MSEE as a function of OSNR in the absence of CFO.

Figure 6 shows measured BER with or without CFO compensation in a homodyne system. The CFO estimation error did not lead to BER degradation because CPE estimation and compensation using pilot subcarriers, compensated for the phase rotation caused by the residual CFO. At around BER of 3.8×10^{-3} , which is an advanced 7% FEC threshold [13], the measured BER showed that the OSNR penalty of the proposed algorithm was small.

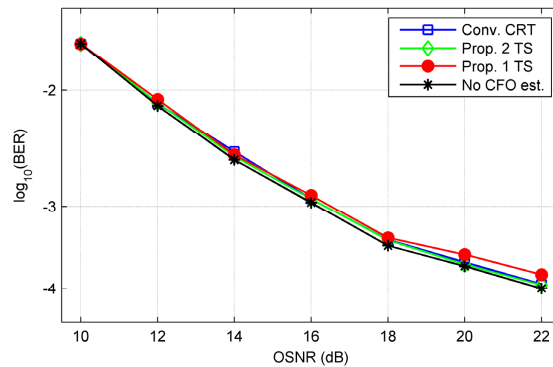


Fig. 6. BER as a function of OSNR in the absence of CFO.

4.3 Experimental CFO Estimation in the presence of CFO

Figure 7 shows the estimation range of CRT-based CFO algorithms, and the difference between the estimated and monitored CFO within the estimation range. For comparison, the performance of the CFO algorithm [8], with the estimation range of a quarter of sampling frequency, was obtained. All algorithms satisfied the expected estimation ranges. The CRT-based algorithms, in particular, had estimation ranges from -5 GHz to 5 GHz which is the same as the sampling frequency. Since angle arithmetic in Eq. (2) for the CFO estimation has circular nature, it is basically a modular arithmetic. As expected from this algorithm, the estimation error of out of estimation range was about the estimation range as shown the Fig. 7.

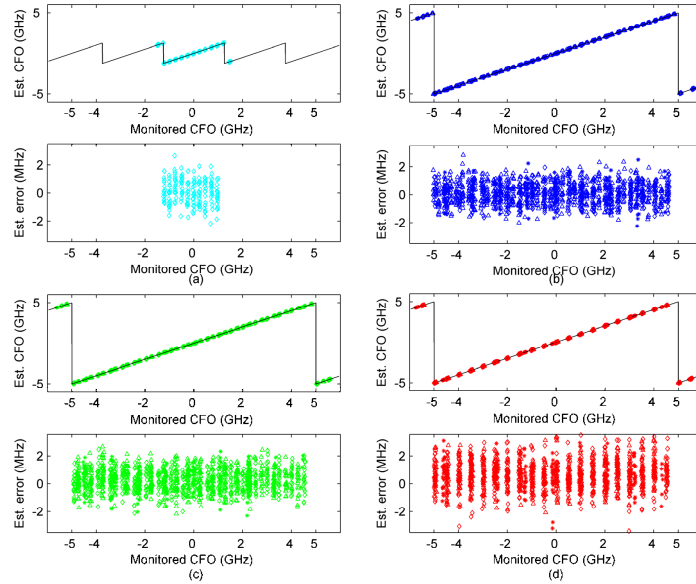


Fig. 7. Estimated CFO and estimation error as a function of monitored CFO; (a) Zhou's algorithm [8] with the sample interval of four; (b) previous CRT-based algorithm; (c) proposed algorithm with two training symbols; (d) proposed algorithm with one training symbol. The real lines are the expected CFO values.

The MSE of CFO and the BER as a function of monitored CFO, were obtained for the previous CRT-based CFO algorithm and the proposed algorithm as shown in Fig. 8 and Fig. 9, respectively. To vary the given CFO, the wavelength of the ECL was swept from 1550.0490 nm to 1550.1390 nm in steps of 0.0090 nm. The results showed that MSE was independent of frequency offset. Also, the estimation error of proposed algorithm with one training symbol was higher than the algorithms with two training symbol due to the shorter sample interval L . However, the small increase of MSE did not affect the BER as shown in Fig. 9.

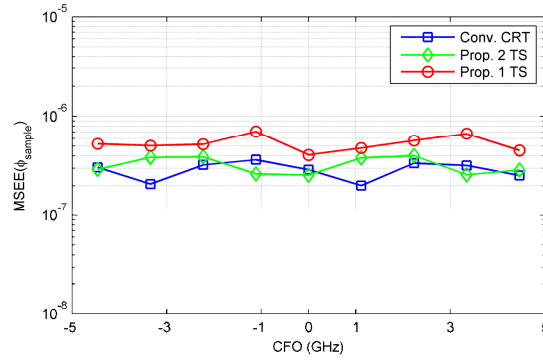


Fig. 8. MSEE as a function of monitored CFO.

The results showed that the BER of all CRT-based CFO algorithms was almost the same and the BER gradually increased as the magnitude of the CFO increased. The BER increases seemed to come from the non-flat frequency responses rather than the CFO estimation error. Also, the CFO out of estimation range did not lead to an abrupt increase in BER because of the sampling effect and modular characteristics of CFO estimation algorithm. Sampling at the receiver caused aliasing effect and thus, in-band image signal had shifted CFO. Also, the estimated CFO value would be shifted due to the modular characteristic of CFO algorithm. Since both of shifted frequencies were the same as sampling frequency, there was no abrupt increase in BER. In a high OSNR condition, there were two humps on the sides of the zero CFO, which may come from DC offset. DC offset could affect the BER in the presence of CFO [18] and the residual DC offset after compensation could deteriorate the subcarrier which was shifted to DC due to CFO.

Experimental results of MSEE of CFO and BER showed that the proposed algorithm had the estimation range of sampling frequency and BER degradation due to short training symbol was negligibly small.

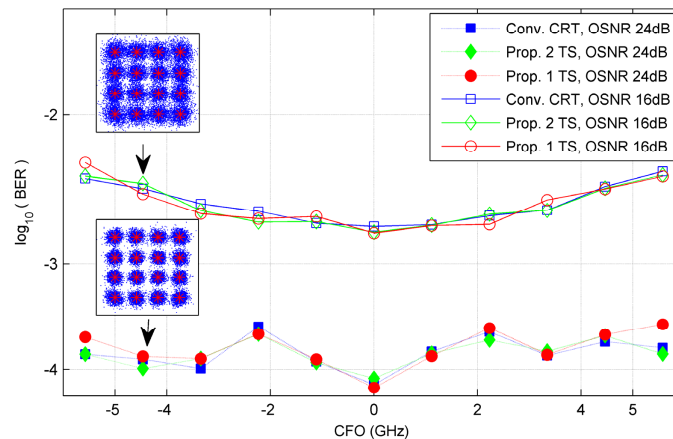


Fig. 9. BER as a function of monitored CFO.

5. Conclusion

We proposed a novel CRT-based CFO algorithm for wide range CFO estimation with a simple, short training symbol structure. By adopting a single frequency training symbol for the modified CRT-based algorithm, the restriction on the training symbol structure was released and the required number of training symbols could be decreased. The validity of the

algorithm was confirmed by numerically and experimentally demonstrating the BER and estimation error as a function of OSNR and frequency offset in a 16-QAM CO-OFDM system. The simulation of 112 Gbps transmission over an 800 km SSMF with 16 PDM-QAM showed the CFO estimation in CRT-based algorithms had a full-range corresponding to the sampling frequency. Experimental results in 16-QAM CO-OFDM system were consistent with the simulation. The results also showed that BER degradation of the proposed algorithm with one training symbol was small despite the shorter training symbol. In addition, the experimental results showed that the accuracy of the time domain CFO estimation was limited not by ASE but by the laser linewidth. We numerically and experimentally showed the feasibility of the proposed algorithm for estimation of CFO in a practical CO-OFDM system.

Acknowledgments

This work was supported by the IT R&D Program of MKE/KEIT (KI002037, coherent optical OFDM technologies for next generation optical transport networks), Republic of Korea.